

Effect of Aluminum on the Structural, Optical, Electrical and Photovoltaic Properties of ZnSe/n-Si Heterojunction Solar Cell

Hanan K. Hassun, Hiba M. Ali, Shaymaa Qasim Abdul Hasan and Samir A. Maki
Department of Physics, College of Education for Pure Science (Ibn Al-Haitham),
University of Baghdad, Baghdad, Iraq

Abstract: Aluminum doped Zinc Selenide ZnSe/n-Si thin films of (250±20 nm) thickness with (0.01, 0.02 and 0.03) are depositing on the two type of substrate (glass and n-Si) to manufacture (ZnSe/n-Si) solar cell through using thermal vacuum evaporation procedure. Physical and optoelectronic properties were examined for the samples. X-ray and AFM techniques are using to study the structure properties. The energy band gap of as-deposited ZnSe thin films for changed dopant ratio were ranging from (2.6-2.68 eV). The results of Hall effect show that pure and doping films were (p-type) and the concentration of the charge carriers and the carriers mobility increases with increase Al-dopant ratio. The (C-V) measurement have shown that the heterojunction were of abrupt type. In addition, the I-V characteristics of ZnSe/Si heterojunctions show the forward dark current varies with applied voltage, besides the saturation current and the ideality factor are determined under different doping percentage. Also, the (I-V) characteristic for ZnSe/Si heterojunction show that the forward current at dark varies with applied voltage and the I_{sc} and V_{oc} have been studied. The photoelectric properties designated an increase light current of heterojunctions with cumulative Al-dopant and I-V characteristics under illumination showed that the heterojunction (ZnSe: Al (0.3%)/Si) have a high efficiency.

Key words: ZnSe, solar cell, C-V measurement, Al dopant, X-ray, photoelectric

INTRODUCTION

Zinc selenide thin films studied for last few decades, thus far, these materials present scientifically attention largely by reason of their technology significant requests. Amongst these submissions are optoelectronic devices for instance blue light emitting diodes, photodiodes, electroluminescent devices, etc. Antohe *et al.* (2013) ZnSe belongs to 2-6 semiconductor family, it has direct band-gap transition (Ismail and Gould, 1989) also ZnSe is a foremost material in the construction of solar cell (Chopra and Das, 1983) where the energy gap is (2.7 eV) at room temperature and that make it suitable applicant for the window layer in the solar cells fabrication (Yang *et al.*, 2013; Mokili *et al.*, 1996; Tripathi *et al.*, 1993).

Diverse techniques utilized for zinc selenide thin films deposition such as Chemical Vapor Deposition (CVD), Chemical Bath Deposition (CBD), vacuum evaporation, radio-frequency assisted magnetron sputtering, Molecular Beam Epitaxy (MBE), etc. (Rumberg *et al.*, 2000; Estrada *et al.*, 1994; El Sherif *et al.*, 1996; Rizzo *et al.*, 2000; Goto *et al.*, 2000). The contact resistance produced via the work function mismatch is typically observing in ZnSe

devices, larger connection resistance will effect in the device presentation degradation which is required to be eliminated for realizing high-performance devices. Doping has establish to be an efficient method which is similarly, a feasible method to tune their optoelectronic properties and further increase their device performances (Javey *et al.*, 2002). Silver (Ag) increases the electrical conductivity attributable to acceptor dopant in 2-6 materials, Bismuth was used as a dopant to make small resistive p-type ZnSe thin films with composite method of doping, silver and Copper (Cu) was doped via ion exchange procedure in 2-6 semiconductor materials. Also, the electrical and the optical properties are important for solar cell applications (Shah *et al.*, 2014). In this research solar cell was fabricated from (p-ZnSe/n-Si) heterojunction which prepared after deposited films thru using thermal evaporation technique from (ZnSe) compound alloy, all thin films have doping with various ratio of Aluminum (Al) and deposited on (n-type) single crystal silicon substrate with orientation (111) in order to study the consequence of doping on structures, optical, electrical then photovoltaic properties, characterization methods and results were investigated and reported.

MATERIALS AND METHODS

Experiments: ZnSe alloy prepared in an evacuated quartz tube, (99.999% pure of zinc and selenide elements, agreement with their atomic percentages evaluated by means of an electronic balance with the slightest count of (10^{-4} g), the material mixed well and placed in the quartz tube (length ~25 cm and internal diameter ~8 mm) which was attached to the evacuated system, then sealed under ($\sim 10^{-3}$) Torr vacuum, then heated for 5 h, the temperature of the furnace was elevated at a degree of ($10^{\circ}\text{C}/\text{min}$). Thin films of ZnSe of thickness about (250 ± 20 nm) were deposited on glass slides and N-type Si wafer substrates, by thermal evaporation utilized (Edwards-Unit 306) system. Also, n-sort Si wafer with crystal orientation (111), energy gap of 1.1eV, diameter 76.2 mm and thickness (508 ± 15) μm were cleaned by put it in dilute 1% HF solution to eliminate native oxide, wash away with deionized water and dried with nitrogen gas. The (1×1 cm² area) was square-shaped of n-type silicon substrate. All thin films have been doped with different ratio of Aluminum (0.01, 0.02 and 0.03). Moreover, the thin film thickness was determined by using an optical interferometer method. Effect of doping have been studied by X-ray diffractions via. (SHIMADZU-Japan-XRD 6000) diffractometer system which records the intensity as a function of Bragg's angle. The surface morphology was studied through (AFM). Also, the optical transmission measurements were calculated by (UV/Visible 1800 spectrophotometer) in the select of wavelength (400-1000 nm). Hall measurement is working via. Van der Pauw (Ecopia HMS-3000) to regulate majority carrier concentrations, kind of carrier and the mobility. The I-J measurement investigated via. (F30-2, Farnell Instrument) and (Keithley digital electrometer 616), the measurement were achieved in dark and light with intensities 100 mW/cm². The C-V measurement for all heterojunction sample are determined by way of (LRC meter GWinstek 8105G) with fix frequency of (100 kHz), to calculate all diverse factors.

RESULTS AND DISCUSSION

Beginning with X-ray diffractions the scanning angle 2θ was varied in the range of (10 - 80°) in order to know the crystal structure. Figure 1 show the XRD patterns of ZnSe thin films per diverse ratio of aluminum (0.01, 0.02 and 0.03), it is clear that all ZnSe thin film are polycrystalline per cubic phases and high sharp peak conforming to (111) plane and diffraction peaks can be assigned to zinc blende ZnSe (JCPDS 37-1463) besides no noticeable impurity phases. Moreover, we can obvious two peaks (220) and (311) where the situations of the measuring diffraction peaks prepare not variation meaningfully but the intensities of the peaks change.

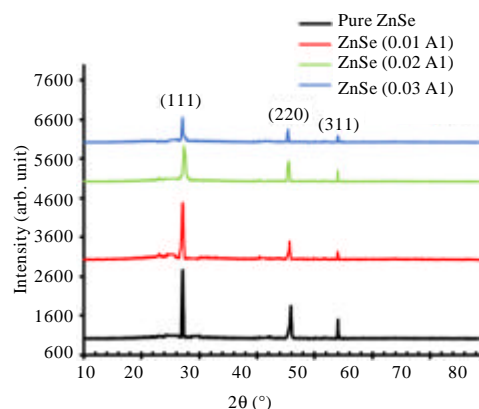


Fig. 1: X-ray diffraction form of (ZnSe) films for different Al ratio

Table 1: X-ray diffraction parameters for pure and doping ZnSe thin films

ZnSe (250 nm)	$2\theta(^{\circ})$	$d_{\text{exp}}(\text{\AA})$	FWHM ($^{\circ}$)	$C_s(\text{nm})$
Pure	27.065	3.291807	0.342	24.97124
0.01 Al	27.092	3.291667	0.361	23.65453
0.02 Al	27.111	3.290261	0.409	20.87759
0.03 Al	27.123	3.286049	0.434	19.67577

Table 2: Grain size and roughness for pure and doping ZnSe thin films

ZnSe	Grain Size (GS)(nm)	Roughness (nm)	rms (nm)
Pure	115.20	9.8	13.20
0.01 Al	97.31	11.6	18.30
0.02 Al	87.86	16.3	22.11
0.03 Al	81.39	23.5	38.34

Slight aluminum atom dopant in flowing to the lattice structure then touching to interstitial situations in ZnSe, the (Ionic Radius) of impurity atom play an important role which indicated that Al diffused interstitially. From Scherrer's equation we can calculate the crystallites size (Culity, 1978).

$$C.S = (0.94\lambda) / ((FWHM)\cos\theta) \quad (1)$$

The (λ , FWHM and θ) are wavelength of radiation, full width half maxima of the main peak and the diffraction angle, respectively.

Table 1 demonstrates the crystallite size for pure and doping samples and we can recognize the value reductions by means of the Al percentage rises by reason of the relatively small atom doping toward the inside to the lattice structure and moved to interstitial position in the ZnSe, results were gotten agreement with other studies (Shah *et al.*, 2014; Yim *et al.*, 2009).

Figure 2 and Table 2 show images in two-dimensional and the three-dimensional surface morphology (AFM) and the values of the grain size, roughness and root mean square of ZnSe thin films pure and doping with different ratio, respectively.

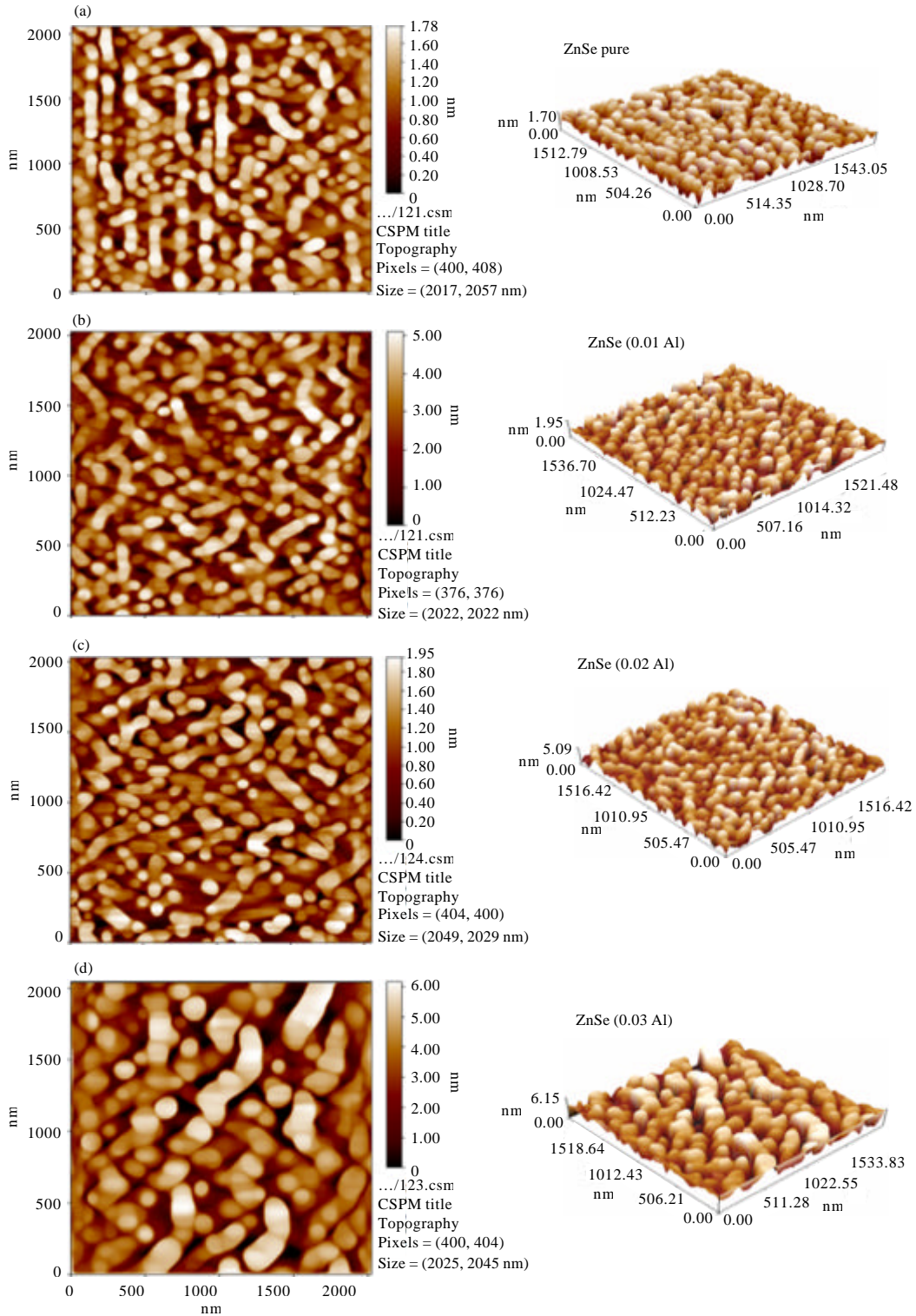


Fig. 2: Surface morphology images AFM of ZnSe thin films for pure and different doping ratio

From all film images one can see change in the morphology of the film when doping with aluminum and

the surface roughness intensification with increasing Al ratio, small amount of defects shows good crystallinity in

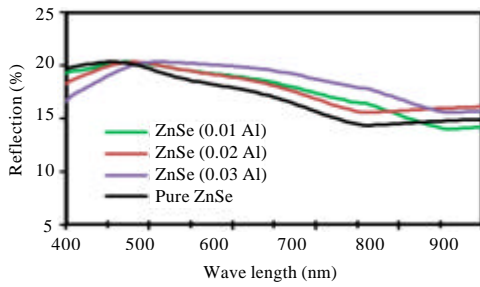


Fig. 3: The reflection spectrum of pure ZnSe thin films and doping

grown ZnSe thin films. The large values of surface roughness indicates the possibility to use these films in solar cell or use it as a cover antireflection coating as it reduces light reflection and increases film absorption for energy photons in the visible region of the electromagnetic spectrum, similar behavior has reported by other Su *et al.* (1999).

With the intention of appreciate the optical parameters of ZnSe thin films were measured reflectance spectra at standard incidence of light on the samples surface. Also, the absorption coefficient (α) and the optical energy gap can be calculate as of that equations (Hassun, 2017).

$$\alpha = (2.303)(A)/(t) \quad (2)$$

$$\alpha h\nu = \beta(h\nu - E_g)^r \quad (3)$$

Where (A, t, β , $h\nu$ and E_g) is the absorbance, thickness, constant, the photon energy and the band gap, (r) was constant have value [2.0, 3.0, 1/2, 3/2] reliant on the material besides the kind of the optical transition.

Figure 3 shows reflected spectrum of ZnSe thin films pure and doping with dissimilar ratio where the amount of reflectivity depends on the incident wavelength, the surface roughness and the angle between the incident beam and the surface of the cell, all these factors result on the intensity of reflected beam. The effect of doping change reflection according to wavelength and the reason for this is free hole absorption and effect of packing density and the crystallinity of the films.

Also, Figure 4a, b expression the absorption coefficient and the optical band gap energy of pure ZnSe film and with Al doped films, we find decreasing absorption coefficient through minor photon energy formerly starts a regular increasing to all films with increase energies of the photon in the range of (1.7-2.1) eV and rapidly hard rise over energies that equivalent to or greater than the optical energy gap of all film as a result of a procedure of absorption happens within the variety

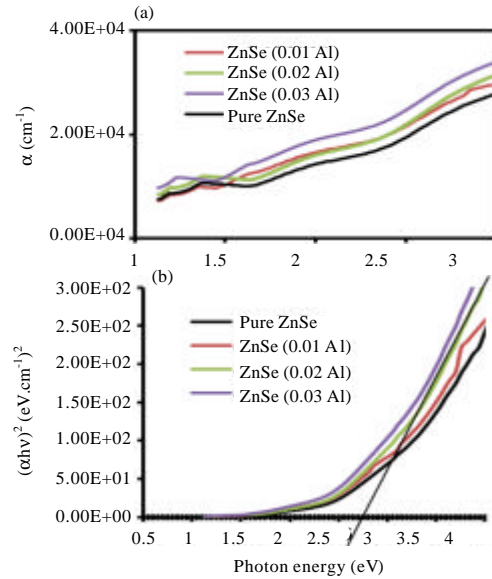


Fig. 4: a, b) The absorption coefficient and the energy gap for pure ZnSe and doping thin films

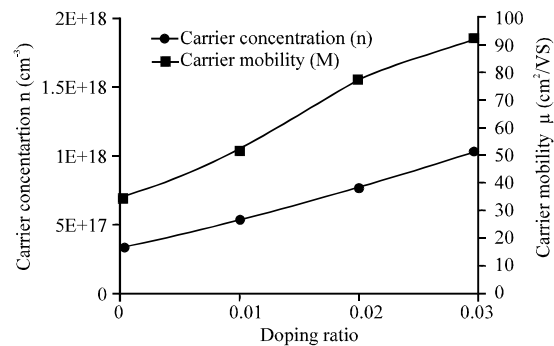


Fig. 5: Variation of carrier concentration and mobility as a function of Al doping ratio

includes the optical absorption edge which may cause due to defects and impurities of the samples. Moreover, Fig. (4b) demonstration the band gap value of pure ZnSe film with Al doped films, the optical band gap value decreased from (2.68, 2.66, 2.64-2.6) eV for pure and doping Al (0.01, 0.02 and 0.03), respectively, associated with the introduction of the Al impurity level between the valance and conduction bands a good agreement have been made from other studies (Shah *et al.*, 2014; Lohar *et al.*, 2016; Aqili *et al.*, 2012).

Figure 5 show carrier concentration in addition Hall mobility, the value the carrier concentration and mobility increase when increasing the Al ratio due to effect of substitution Zn by impurity atom. The redundant holes would decrease the electrical resistivity and increase the carrier concentration. From Hall measurements the positive insignia of Hall coefficient directs that the

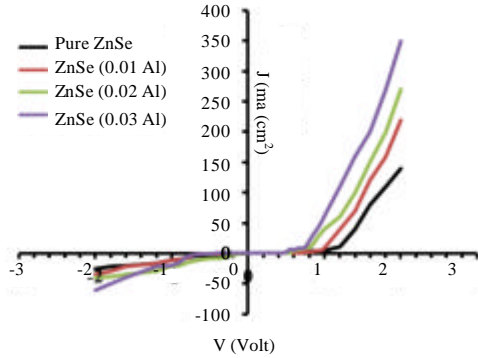


Fig. 6: Current-voltage designs for ZnSe/Si solar cell under dark for pure and different Al ratio

Table 3: Hall parameters for pure and doping ZnSe thin films

ZnSe	Hall coefficient	Mobility (cm ² /V.S)	Carrier concentration n (cm ⁻³)	Resistivity (Ω cm)
Pure	19.031161490	34.77	3.28409E+17	5.47E-01
0.01 Al	11.663790470	51.64	5.35846E+17	2.26E-01
0.02 Al	8.211752892	77.22	7.61104E+17	1.06E-01
0.03 Al	6.108862947	92.41	1.0231E+18	6.61E-02

conductivity nature of the film is p-type. Table 3 show the electrical resistivity for doped ZnSe films is lower than that of the pure ZnSe film this is because of the improved film structure, reduce defect centers and grain boundary defects, therefore, the carrier mobility improves, similar result is agreement with (Shen *et al.*, 2008; Zhang *et al.*, 2012)

Figure 6 signifies the (Current-Voltage I-V) curve of ZnSe/Si heterojunction solar cell below dark and illumination conditions in the forward and reverse bias with altered ratio of aluminum.

The I-V curves of pure and doping heterojunction under the forward bias condition show the reverse currents are very weak and the exponential rise at low voltage for the forward currents. This is as a result of the lessening in the breadth of depletion region by increasing in the majority carrier injects via the applying voltage and that make possible the decrease in the built-in potential, then as the bias is increased the forward current increases. Also, the forward current increased with surges dopant ratio of Al caused by the increase of carrier concentration after incorporation of impurity atoms (Chen and Chang, 2008). Under dark and light condition the characteristics is explanation thru the equation (Hassun, 2018).

$$I = I_s \left(\exp \left(\frac{qV}{\beta K_B T} \right) - 1 \right) - I_L \quad (4)$$

$$\beta = \frac{q}{K_B T} \frac{dV}{d(\ln I)} \quad (5)$$

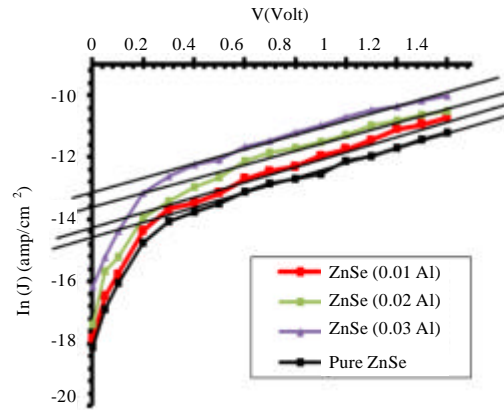


Fig. 7: ln (J) contrasted with voltage for the fabricated ZnSe/Si heterojunction in dark

Table 4: β, J_s and Φ_b values for pure and doping ZnSe/Si heterojunction

ZnSe (250 nm)	Ideality factor	(J _s)(A/cm ²)	(Φ _b)(eV)
Pure	2.156985	1.56E-07	0.825393
0.01 Al	1.950002	2.84E-07	0.809876
0.02 Al	1.865219	3.40E-06	0.745578
0.03 Al	1.771103	4.70E-06	0.737192

where, (I_s, I_L, I, V, T, K_B, q and β) were saturating current, light currents, the total current, applying, temperature, Boltzmann constant, electron charge and the ideality factor, respectively. The pattern of (ln J) versus V (forward bias) of heterojunction show in Fig. 7 the calculation of the ideality factor, barriers height (Φ_b) in addition the reverse saturation current density show in Table 4.

The ideality factor more than unity can be accredited to the recombination of electrons and holes in the depletion region in addition to the tunneling effect depending on both sides of the heterojunction and on the presence of defect states. Also, we can see the effect of doing in reduction value the of ideality factor, barrier height and increase value of saturation current, this performance credited to improvement of crystal structure. The conversion efficiency and F.F of a solar cell is calculated using equations (Hassun, 2018).

$$\eta = \frac{P_m}{P_{in}} \times 100\% = \frac{I_m V_m}{P_{in}} \times 100\% \quad (6)$$

$$F.F = \frac{J_m V_m}{J_{sc} V_{oc}} \quad (7)$$

Figure 8 and Table 5 shows the V_{oc} and I_{sc} for pure and with Al doped ZnSe/Si heterojunction. It can be seen that the V_{oc} and I_{sc} increase with doping. From the results of Hall effect measurement, the carrier concentration increases with doping, accordingly, V_{oc}

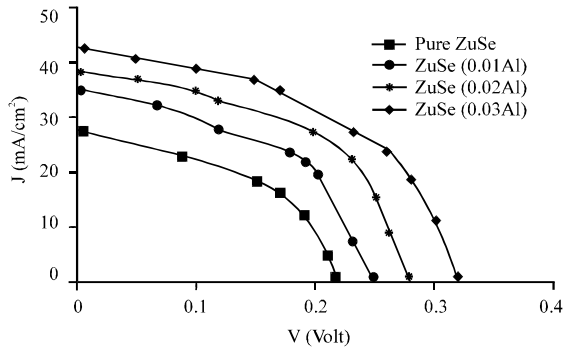


Fig. 8: I-V characteristic for ZnSe/Si solar cell under illumination (100 mW/cm² white lamp) for pure and Al dopant

Table 5: The solar cells characterization for ZnSe/Si junctions pure and with Al dopant.

ZnSe	V _{oc} (Volt)	J _{sc} (mA/cm ²)	V _{max} (volt)	J _{max} (mA/cm ²)	FF	η (%)
Pure	0.22	30	0.11	14	0.233333	1.54
0.01 Al	0.25	38	0.13	17	0.232632	2.21
0.02 Al	0.28	42	0.15	21	0.267857	3.15
0.03 Al	0.32	46	0.18	26	0.317935	4.68

Table 6: Value of C₀, W, V_{bi} and N_A, for pure and doped ZnSe/Si junctions

ZnSe	C ₀ (mf/cm ²)	W=ε _s /C ₀ (nm)	V _{bi} (Volt)	N _A (cm ⁻³)
Pure	87.7	55.5	0.9	1.44E+16
0.01 Al	84.5	57.6	0.95	2.83E+16
0.02 Al	72.5	67.2	1.05	3.56E+16
0.03 Al	60.8	80.13	1.15	4.66E+16

where, (N_d, N_p, ε_n, ε_p, V_{bi} and V) are the donor concentrations, the dielectric constant of n type semiconductors, the dielectric constants of p type semiconductors, the built-in junction potential and the applied voltage:

$$W = \frac{\epsilon_s}{C_0} \tag{9}$$

The C₀ capacitance at zero biasing voltage and (ε_s) was dielectric constant of heterojunction. The C-V measurements show that the capacitance of the heterojunction is lessened with an rise in the reverse bias and an approximately linear (1/C² against V_{bi,as}) relationship then show the heterojunction of abrupt type. Also, Table 6 indication to the effect of impurity which may explaining by the extension of depletion layer with the V_{bi}. The dopant atoms have better-quality of electrical characteristics where decrease resistivity and increase connectivity.

CONCLUSION

We synthesized pure and Al doped ZnSe thin films successfully using thermal evaporation method. The XRD analysis displays that wholly the deposited films were polycrystalline and the crystallite size was highly oriented in (111) direction. The optical transitions in ZnSe was direct and value of optical energy gap reductions througha dding impurity. The capacitance drops by increased of the reverse bias voltage and the best values of the width of the depletion layer and the V_{bi} at doping ratio (0.03 Al). Also, the 1-5 measures of heterojunction device examined for rectifying behaviors, the value of ideality factor discounts with doping. 1-5 characteristic below illumination were approved by incident power density identical to (100 mW/cm²), the maximum values of efficiency (4.68%) for doping ratio(0.03Al).

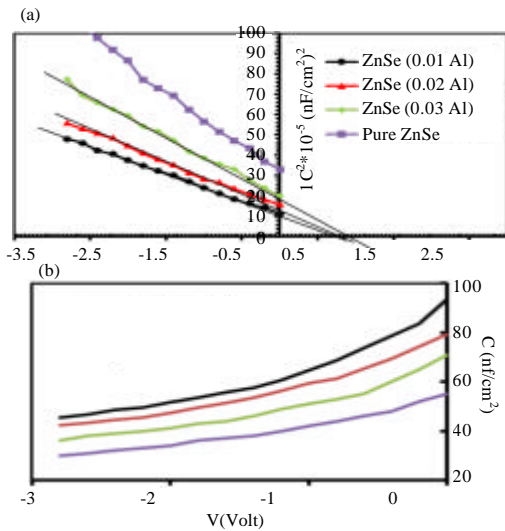


Fig. 9: The disparity of: a) capacitance and b) 1/C² as a function of reverse bias voltage for pure and doped ZnSe/Si junctions

was also enhanced. Besides, the carriers under the action of built-in potential would result in the big I_{sc}. Also, the efficiency increases with doping due to improve the increase the absorption coefficient and charge carriers (Ikhmayies and Ahmad-Bitar, 2008).

Also, the potential barrier at the junction can demonstrated through (Capacitance-Voltage C-V) characteristics. Figure 9a, b presents the C-V characteristics in the reverse bias region at (100 kHz) intended of pure and Al dopant p-ZnSe/n-Si heterojunction, the junction capacitance for each unit area is calculating from expression.

$$C = \left[\frac{q\epsilon_n\epsilon_p N_n N_p}{2(\epsilon_n N_n + \epsilon_p N_p)} \right]^{1/2} (V_{bi} - V)^{-1/2} \tag{8}$$

REFERENCES

- Antohe, S., L. Ion, M. Girtan and O. Toma, 2013. Optical and morphological studies of thermally vacuum evaporated ZnSe thin films. *Rom. Rep. Phys.*, 65: 805-811.
- Aqili, A., Z. Ali and Z. Hussain, 2012. Optical and structural properties of silver doped ZnSe thin films prepared by CSS and ion exchange process. *Proceedings of the 2012 International Conference on Thin Film Solar Technology IV* Vol. 8470, October 10, 2012, International Society for Optics and Photonics, Bellingham, Washington, USA., pp: 1-8.
- Chen, M.Y. and C.C. Chang, 2008. The study of ZnSe/GaAs MSM photodetector using selective-area epitaxy method. *Proceedings of the 2008 3rd International Conference on Sensing Technology ICST*, November 30-December 3, 2008, IEEE, Tainan, Taiwan, ISBN:978-1-4244-2176-3, pp: 289-291.
- Chopra, K.L. and S.R. Das, 1983. Why Thin Film Solar Cells?. In: *Thin Film Solar Cells*, Chopra, K.L. and S.R. Das (Eds.). Springer, Boston, Massachusetts, USA., ISBN:978-1-4899-0420-1, pp: 1-18.
- Culity, B.D., 1978. *Elements of X-ray diffraction*. 2nd Edn., Addison-Wesley, Boston, Massachusetts, USA., ISBN:9780201011746, Pages: 555.
- El Sherif, M., F.S. Terra and S.A. Khodier, 1996. Optical characteristics of thin ZnSe films of different thicknesses. *J. Mater. Sci. Mater. Electron.*, 7: 391-395.
- Estrada, C.A., P.K. Nair, M.T.S. Nair, R.A. Zingaro and E.A. Meyers, 1994. Chemical bath deposition of ZnSe and CuSe thin films using N, N-dimethylselenourea. *J. Electrochem. Soc.*, 141: 802-806.
- Goto, H., T. Ido and A. Takatsuka, 2000. Electrical properties of Sb-doped ZnSe grown by metalorganic vapor phase epitaxy. *J. Crystal Growth*, 214: 529-532.
- Hassun, H.K., 2017. Study of photodetector properties ZnTe: Al/Si prepared by thermal evaporation. Ph.D Thesis, College of Education for Pure Science, University of Baghdad, Baghdad, Iraq.
- Hassun, H.K., 2018. Study the physical and optoelectronic properties of silver gallium indium selenide AgGaInSe₂/Si heterojunction solar cell. *AIP. Conf. Proc.*, 1968: 020017-020017.
- Ikhmayies, S.J. and R.N. Ahmad-Bitar, 2008. Effect of film thickness on the electrical and structural properties of CdS: In thin films. *Am. J. Applied Sci.*, 5: 1141-1143.
- Ismail, B.B. and R.D. Gould, 1989. Structural and electronic properties of evaporated thin films of Cadmium Telluride. *Phys. Status Solidi A.*, 115: 237-245.
- Javey, A., H. Kim, M. Brink, Q. Wang and A. Ural *et al.*, 2002. High-dielectrics for advanced carbon-nanotube transistors and logic gates. *Nat. Mater.*, 1: 241-246.
- Lohar, G.M., R.K. Kamble, S.T. Punde, S.T. Jadhav and A.S. Patil *et al.*, 2016. Electrochemical synthesis of Ni doped ZnSe thin film for photoelectrochemical cell application. *Mater. Focus*, 5: 481-484.
- Mokili, B., Y. Charreire, R. Cortes and D. Lincot, 1996. Extended X-ray absorption fine structure studies of zinc hydroxo-sulphide thin films chemically deposited from aqueous solution. *Thin Solid Films*, 288: 21-28.
- Rizzo, A., M.A. Tagliente, L. Caneve and S. Scaglione, 2000. The influence of the momentum transfer on the structural and optical properties of ZnSe thin films prepared by rf magnetron sputtering. *Thin Solid Films*, 368: 8-14.
- Rumberg, A., C. Sommerhalter, M. Toplak, A. Jager-Waldau and M.C. Lux-Steiner, 2000. ZnSe thin films grown by chemical vapour deposition for application as buffer layer in CIGSS solar cells. *Thin Solid Films*, 361: 172-176.
- Shah, N.A., M. Abbas, W.A. Syed and W. Mahmood, 2014. Physical properties of silver doped ZnSe thin films for photovoltaic applications. *Iran. J. Energy Environ.*, 5: 87-93.
- Shen, Y., N. Xu, W. Hu, X. Xu and J. Sun *et al.*, 2008. Bismuth doped ZnSe films fabricated on silicon substrates by pulsed laser deposition. *Solid State Electron.*, 52: 1833-1836.
- Su, C.H., S. Feth, M.P. Volz, R. Matyi and M.A. George *et al.*, 1999. Vapor growth and characterization of Cr-doped ZnSe crystals. *J. Crystal Growth*, 207: 35-42.
- Tripathi, L.N., S.K. Mishra and R.N. Singh, 1993. Luminescence in ZnSe doped with Pr and (Sn, Pr) phosphors. *Indian J. Pure Appl. Phys.*, 31: 899-903.
- Yang, C.S., Y.P. Hsieh, M.C. Kuo, P.Y. Tseng and Z.W. Yeh *et al.*, 2013. Compressive strain induced heavy hole and light hole splitting of Zn-xCd-xSe epilayers grown by molecular beam epitaxy. *Mater. Chem. Phys.*, 78: 602-607.
- Yim, J.W., D. Chen, G.F. Brown and J. Wu, 2009. Synthesis and *Ex situ* doping of ZnTe and ZnSe nanostructures with extreme aspect ratios. *Nano Res.*, 2: 931-937.
- Zhang, X., K. Man Yu, C.X. Kronawitter, Z. Ma and P.Y. Yu *et al.*, 2012. Heavy P-type doping of ZnSe thin films using Cu₂Se in pulsed laser deposition. *Appl. Phys. Lett.*, 101: 1-3.